

Effect of Ba²⁺ in BNT ceramics on dielectric and conductivity properties

Konapala Sambasiva Rao, Kuan China Varada Rajulu, Bollepalli Tilak, Anem Swathi

Centre for Piezoelectric Transducer Materials, Department of Physics, Andhra University, Visakhapatnam, India;
sambasivaraokonapala@yahoo.co.in; konapala@sify.com

Received 11 December 2009; revised 13 January 2010; accepted 19 February 2010.

ABSTRACT

The polycrystalline (Na_{0.5}Bi_{0.5})_{1-x}Ba_xTiO₃ (x = 0.026, 0.055 & 0.065) (BNBT) ceramics have been synthesized by conventional solid state sintering technique. The tolerance (t) factor of the BNBT composition have been estimated and found to be 0.988, 0.990 and 0.991 for x = 0.026, 0.055 and 0.065 respectively, revealing system is stable perovskite type structure. The compound has a rhombohedral-tetragonal Morphotropic Phase Boundary (MPB) at x = 0.065. XRD results indicated the crystalline structure of the investigated materials are of single phase with rhombohedral structure and the average particle size of the calcined powder is found to lie between 45 nm - 60 nm. The effect of Ba²⁺ on dielectric and conductivity properties in Bismuth Sodium Titanate (BNT) has been studied. The variation of dielectric constant with frequency (45 Hz-5 MHz) and temperature (35°C-590°C) has been performed. The value of T_m and T_d are found to decrease with increase of concentration of Barium in BNT. The value of tanδ in the studied materials is found to be the order of 10⁻² indicating low loss materials. The evaluated Curie constant in the composition is found to be the order of 10⁵ revealing the materials belong to oxygen octahedra ferroelectrics. The theoretical dielectric data of the studied composition have been fitted by using Jonscher's dielectric dispersion relation:

$$\epsilon_r' = \epsilon_\infty + \sin(n(T) \frac{\pi}{2}) \left(\frac{a(T)}{\epsilon_0} \right) (\omega^{n(T)-1}). \text{ The pre-factor}$$

$a(T)$, which indicates the strength of the polarizability showed a maximum at transition temperature (T_m). The exponent $n(T)$ which gives a large extent of interaction between the charge carriers and polarization is found to be minimum in the vicinity of T_m. The A.C. and d.c conductivity activation energies have been evaluated;

the difference in activation energies could be due to the grain boundary effect. The activation enthalpy energies, have been estimated and found to be H_m = 0.37 eV, 0.26 eV and 0.25 eV for BNBT-26, BNBT-55 and BNBT-65 respectively.

Keywords: MPB; Dielectric; Perovskite; Conductivity; Tolerance Factor

1. INTRODUCTION

Recently, according to the stern restriction of environmental pollution such as waste electrical and electronic equipment (WEEE) and restriction of hazardous substance (RoSH), development of lead free piezoelectric ceramics capable of replacing lead-based ceramics is strongly required. The development of lead-free piezoelectric materials has been required. Lead free piezoelectric ceramics have recently attracted great attention for the consideration of environmental protection. Tungsten-Bronze (TB) type, Bismuth Layer-Structured (BLS) type and perovskite type ferroelectrics are known for lead-free piezoelectric ceramics.

Now a days Na_{0.5}Bi_{0.5}TiO₃ (NBT) is considered to be a parent component for lead-free ferroelectric and piezoelectric material [1,2]. But Bi ion is highly volatile at high temperature above 1130°C during sintering and making this material difficult to pole due to its high conductivity [3]. The solution to this problem has been found by many researchers, who were able to modify BNT crystal by the substitution of other A and B-site cations, such as in (Bi_{0.5}Na_{0.5})_(1-1.5x)La_xTiO₃; (BNLT) [4], BNT-KNbO₃(KN) [5], and BNT-Ba(Ti,Zr)O₃ [6] solid-solution ceramic system. The piezoelectric properties of these ceramics were significantly improved.

The piezoelectric property of Na_{1/2}Bi_{1/2}TiO₃-BaTiO₃ (BNBT) system with perovskite structure was studied by B.J. Chu *et al.* [7]. A simple aqueous route was developed for the preparation of (1-x)Na_{1/2}Bi_{1/2}TiO₃xBaTiO₃

by D.L. West *et al.* [8] and studied the crystal structure and dielectric properties. Crystallographically textured ferroelectric and piezoelectric ceramics were prepared by tape casting of slurries containing powder particles with shape anisotropy by T. Kimura *et al.* [9]. $(\text{Na}_{1/2}\text{Bi}_{1/2})_{1-x}\text{Ba}_x\text{TiO}_3$ powders were synthesized by a citrate method, and the piezoelectric and ferroelectric properties of the ceramics were investigated by Q. Xu [10]. $(1-x)\text{BaTiO}_3-x\text{Bi}_{0.5}\text{Na}_{0.5}\text{TiO}_3$ for $x = 0.01-0.3$ ceramics has been prepared by conventional solid state reaction route by Huang *et al.* [11]. Also, crystal structure of the prepared compositions and variation of ϵ' with temperature and $\tan\delta$ at different frequencies have been reported. Barium substituted BNT ceramics have been prepared by the usual double sintering method by Qu *et al.* [12]. The crystal structure of the prepared materials and the effect of Ba^{2+} on the temperature dependence of ϵ' and microstructural by SEM have been reported by the same authors.

It is evident from the above survey that most of the work that has been carried in BNBT system is in its preparative methods, dielectric (variation of ϵ' with temperature only) and piezoelectric properties only. Further, in ferroelectrics in general, the study of electrical conductivity is very important since the associated physical properties like piezoelectricity, pyroelectricity and also strategy for poling are dependent on the order and nature of conductivity in these materials. However, no work on dielectric spectroscopy (frequency dependent ϵ' , $\tan\delta$) and conductivity studies on (BNT-BT) system have been reported in literature. The aim of the present communication is the preparation of $(\text{Bi}_{0.5}\text{Na}_{0.5})_{1-x}\text{Ba}_x\text{TiO}_3$ (BNBT) for $x = 0.026, 0.055$ and 0.065 ceramic compositions and to study the frequency, temperature dependence of dielectric and conductivity properties in the materials with a special emphasis on the Morphotropic Phase Boundary (MPB) of the system.

2. TOLERANCE FACTOR

The concept of tolerance factor (t) is the arrangement of interpenetrating octahedra and dodecahedra in perovskite structure (ABO_3 type) introduced by Goldschmidt, which is given by:

$$\text{tolerance } (t) = \frac{R_a + R_O}{\sqrt{2}(R_b + R_O)} \quad (1)$$

Here, R_a , R_b and R_O are the ionic radii of A, B cations and oxygen respectively, for complex perovskite system R_a and R_b are the ionic radii of composed ions normalized by the atomic ratio. The ionic radii refer to those reported by Shannon [13]. All perovskites have a t value ranging from 0.75 to 1.00. However, it seems that $t = 0.75-1.00$ is a necessary but not a sufficient condition

for the formation of the perovskite structure. The perovskite structure is stable in the region $0.880 < t < 1.090$, [14] and the symmetry is increases as the t value is close 1. The tolerance, t also provides an indication about how far the atoms can move from the ideal packing positions in the structure. It reflects the structural modification such as rotation, tilt, distortion of the octahedral [15]. These structure factors consequently affect the electrical property of the material [16-18]. In the Present BNBT system tolerance factors have been estimated to be 0.988, 0.990 and 0.991 for BNBT-26, BNBT-55 and BNBT-65 respectively. The tolerance factors in the studied materials are found to lie well within the limit indicating the materials belong to stable perovskite structure.

3. EXPERIMENTAL

Starting materials, analar grade oxides and carbonate powders of Bi_2O_3 , TiO_2 , BaCO_3 , Na_2CO_3 were weighed according to the formula, $(\text{Bi}_{0.5}\text{Na}_{0.5})_{1-x}\text{Ba}_x\text{TiO}_3$ ($x = 0.026, 0.055$ & 0.065). The weighed powers were mixed well in methanol medium using agate mortar. An extra amount of 3 wt% Bi_2O_3 and Na_2CO_3 were added to the initial mixture to compensate the losses of bismuth and sodium at high temperature. The resultant grounded mixture was calcined at 850°C for 2 hr with intermediate grinding. After calcination, the ceramic powder was mixed with polyvinyl alcohol (5%), as the binder and then pelletized into discs, 13 mm diameter and about 1.1-1.5 mm thickness. After binder burnout, at 600°C for 1 hr, the green discs have been sintered in a closed platinum crucible at $1150^\circ\text{C}/4$ hr. Silver paste was fired on both the surfaces of the disc as an electrodes for electrical measurements. The phase purity of the final product was confirmed via the X-ray diffraction (XRD) using $\text{CuK}\alpha$ radiation. The densities of the sintered pellets have been determined by the liquid displacement/Archimedes method. The measurement of dielectric constant (ϵ'), loss tangent ($\tan\delta$) and conductivity (σ) as a function of temperature from RT to 590°C in the frequency range of 45 Hz - 5 MHz using HIOKI 3532-50 LCR Hi-tester, Japan with heating rate of $5^\circ\text{C}/\text{min}$ offset temperature 0.2°C and time period of 1 min for making the above measurements. Following are the chosen compositions which are well below, near and within MPB region.

$(\text{Bi}_{0.5}\text{Na}_{0.5})_{0.974}\text{Ba}_{0.026}\text{TiO}_3$ - BNBT-26 (well below MPB).

$(\text{Bi}_{0.5}\text{Na}_{0.5})_{0.945}\text{Ba}_{0.055}\text{TiO}_3$ - BNBT-55 (Near MPB).

$(\text{Bi}_{0.5}\text{Na}_{0.5})_{0.935}\text{Ba}_{0.065}\text{TiO}_3$ - BNBT-65 (Within MPB).

4. RESULTS AND DISCUSSION

4.1. XRD Analysis

X-ray diffractograms of $(\text{Bi}_{0.5}\text{Na}_{0.5})_{1-x}\text{Ba}_x\text{TiO}_3$ ($x = 0.026,$

0.055 and 0.065) compositions with 2θ values from 10° to 70° along with BNT are shown in **Figure 1**. The structure and lattice parameters of BNBT materials have been determined by using a standard computer program "POWD" (interpretation and indexing program by E. Wu, school of physical sciences, Flinders University of South Australia, Bed Ford Park, Australia). It is obvious from the **Figure 1** all the peaks in the XRD pattern of the BNBT are correspond to the BNT (3.886\AA) phase with rhombohedral structure as reported by different researchers [19-21]. All the XRD peaks obtained in compositions are indexed and found to be single phase with rhombohedral structure. XRD pattern of the compositions showed an extra peak, indicating a possible presence of some unidentifiable extra phase due to non-miscibility of substituted ions with the host lattice ion [22]. It is evident from the **Figure 1** that the substitution of Ba^{2+} in BNT shifts the peak position towards lower angle side. Also, the substitution of Ba^{2+} in BNT for $x > 0.055$ resulted in a splitting of the (2 0 0) peak into two peaks of (0 0 2) and (2 0 0) reflections. This splitting is obvious at $x = 0.065$ and can be clearly seen in the extended XRD pattern of the corresponding material at 2θ in the range 42° to 49° (**Figure 1(b)**). Splitting in the peak position reveals the composition BNBT-65 is well in MPB region where rhombohedral and tetragonal phase co-exist. The above results are found

to be very good agreement with previous work on $(1-x)(\text{Bi}_{0.5}\text{Na}_{0.5})\text{TiO}_3-x\text{BaTiO}_3$ [23,24]. Using lattice parameters theoretical densities (ρ_{theor}) of the compositions are evaluated. Average particle size of the calcined powders of the composition is determined using Debye-Scherrer formula. Calculated values of lattice parameters, density, average particle size, average grain size and porosity are given in **Table 1**.

It is seen from the **Table 1** that as increasing the Ba content the lattice parameters of the BNBT materials are found to increase whereas the lattice distortion decreases. The experimental densities are found to be 5.87 g/cm^3 , 5.98 g/cm^3 and 5.91 g/cm^3 for $x = 0.026$, 0.055 and 0.065 respectively which are 97.2%, 98.9% and 97.8% to that of theoretical value indicating the materials are high dense. Further, an average particle size in the calcined powders is found to be in nanometer range.

4.2. SEM and EDS

In the present Ba substituted BNT compositions experimental density is found to be more than 97% to that of the theoretical one, reveals less porosity. **Figure 2** shows the SEM micrographs on studied compositions. It is seen from the **Figure 2** spherical shape grains with an average grain size $1.25\text{ }\mu\text{m}$, $1.01\text{ }\mu\text{m}$ and $1.09\text{ }\mu\text{m}$ found in BNBT-

Table 1. Lattice parameters and related properties of BNBT ceramics.

Composition	Lattice Parameters/ distortions		Density (ρ)(g/cm^3)			Avg. particle size (nm)	Avg. grain size (μm)	Porosity
	a (\AA)	α (angle)	ρ_{exptl}	ρ_{theor}	Density %			
BNBT-26	3.886	89.894	5.87	6.04	97.2	47	1.25	0.028
BNBT-55	3.891	89.891	5.98	6.04	98.9	56	1.01	0.011
BNBT-65	3.892	89.890	5.91	6.04	97.8	48	1.09	0.022

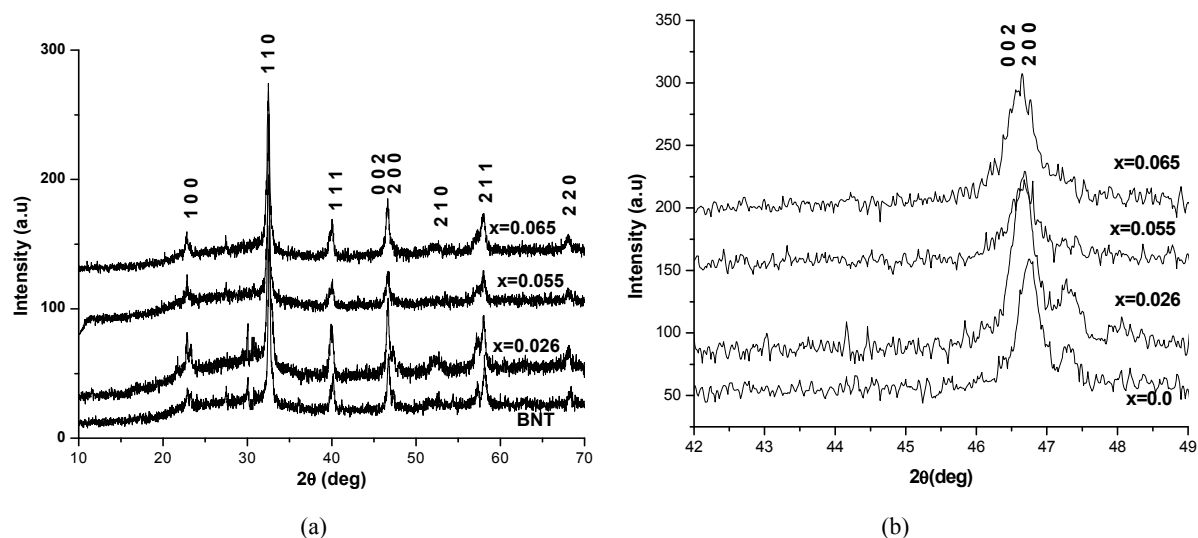


Figure 1. X-ray diffractograms on BNBT system (a) 2θ , 10° - 70° ; (b) 2θ , 42° - 49° .

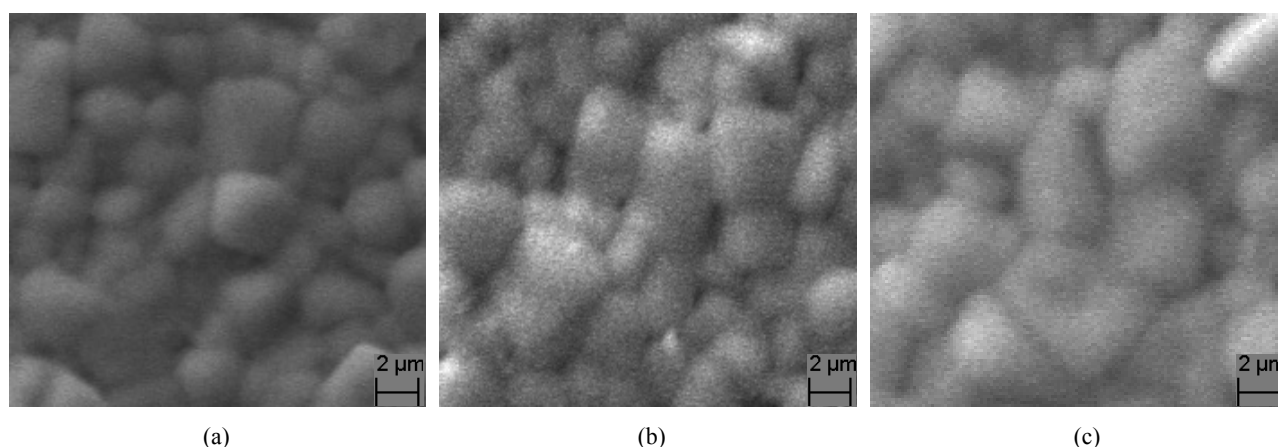


Figure 2. SEM micrographs of (a) BNBT-26; (b) BNBT-55; (c) BNBT-65.

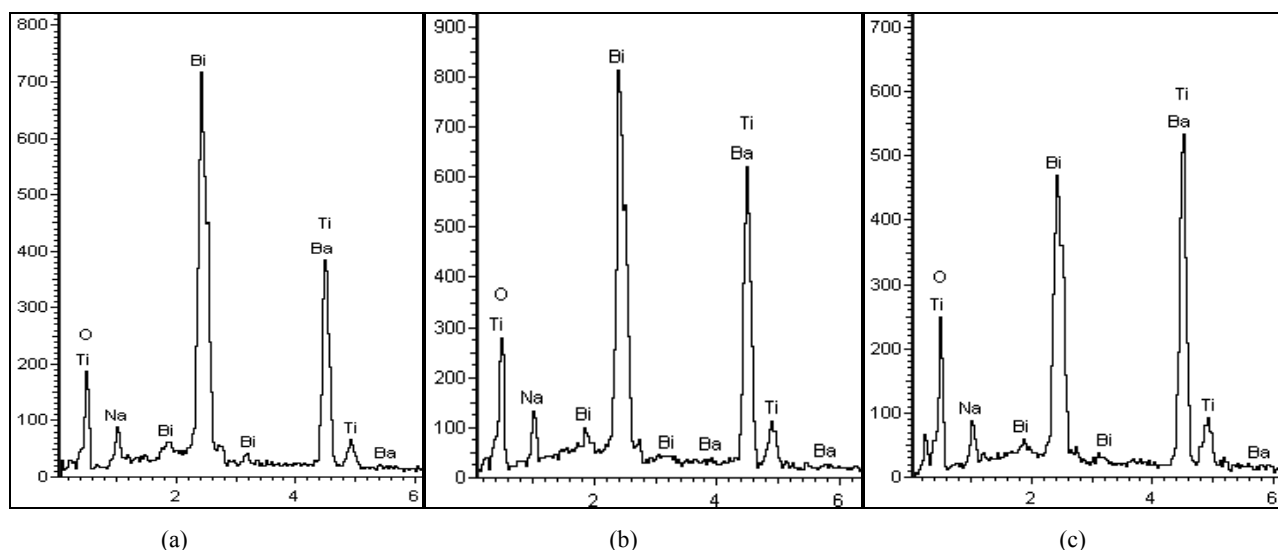


Figure 3. Energy dispersive X-ray spectrums. (a) BNBT-26; (b) BNBT-55; (c) BNBT-65.

Table 2. Dielectric properties of BNBT ceramics.

Composition	Dielectric constant(ϵ') (1 kHz)		T_d ($^{\circ}\text{C}$)	T_m ($^{\circ}\text{C}$)	$\tan \delta$ (1 kHz)		Conductivity (σ)(1 kHz)	Curie Constant ($\times 10^5$) $^{\circ}\text{K}$	n(T)	log A(T)
	RT	T_m			RT	T_m				
BNBT-26	541	1625	180	318	0.059	0.05	1.38×10^{-8} (s/cm)	1.35	0.285	-9.4
BNBT-55	818	1891	140	313	0.04	0.02	2.02×10^{-8} (s/cm)	1.51	0.184	-3.5
BNBT-65	701	1233	100	305	0.06	0.02	2.46×10^{-8} (s/cm)	1.0	0.19	-3.6

26, BNBT-55 and BNBT-65 respectively.

Energy Dispersive X-ray Spectroscopy (EDS) is a chemical microanalysis technique used in conjunction with SEM and is not a surface science technique. The EDS technique detects X-rays emitted from the sample during bombardment by an electron beam to characterize the elemental composition of the analyzed volume. **Figure 3** shows the EDS of Ba substituted BNT compositions. The spectrum (**Figure 3**) shows the elements present in the prepared compositions are Na, Bi, Ba, Ti and O only.

4.3. Dielectric

The temperature dependence of dielectric constant ϵ' and dielectric loss $\tan \delta$ of Ba substituted BNT system at 1 kHz are shown in **Figure 4**.

It is seen from **Figure 4(a)** that two dielectric peaks have been observed in each composition. The observed two dielectric peaks can be attributed to the factors caused by the phase transitions from ferroelectric to anti-ferroelectric, which is called depolarization tempera-

ture (T_d) and from anti-ferroelectric to paraelectric phase, at which the maximum value of dielectric constant corresponding temperature is Curie temperature (T_m) (**Figure 4(a)**). The value of T_d and T_m are found to decrease with increasing the concentration of Ba, indicating the conductivity of the materials is decreased compared with BNT. These results are consistent with previous reports on BNT, BNT-BT, BNT-KBT, BNKLT lead free ferroelectric systems [25-31]. Also it is obvious from the **Figure 4** at high temperatures another dielectric maxima is observed at 520°C in the compositions. The observed anomaly may be related to the relaxation mechanism in the samples [32]. It is seen from **Table 2** considerable increase in the value of room temperature dielectric constant (ϵ'_{RT}) as well as at Curie temperature (ϵ'_{T_m}) are observed in the compositions for $x = 0.026$ and 0.055 having rhombohedral structure. Whereas decrease in the value of ϵ'_{RT} and ϵ'_{T_m} are observed in the composition for $x = 0.065$ which is in MPB region where rhombohedral and tetragonal phase coexist. The value of dielectric loss ($\tan \delta$) in the compositions is found to be the order of 10^{-2} indicating the low loss materials. The important mechanism of conductivity in these ceramics is the movement of ions present in the current carrying conductor. It is well known reason that the alkali ions are good current carriers in ceramics; because these ions play an important role in the conductivity of BNBT ceramics. The Na^+ ions in BNT move easily upon heating, resulting in increase in conductivity with increasing temperature. The present Ba substituted ceramics, Ba^{2+} (large ion) occupies the A-site of BNT, which possibly blocks the passage of Na^+ current carriers. When the temperature is increased above T_m , the value of $\tan \delta$ is found to increase drastically. Curie constant in the

compositions have been evaluated and found to be the order of 10^5 K indicating the materials belong to oxygen octahedra ferroelectrics [33]. The value of ϵ'_{RT} , ϵ'_{T_m} , $\tan \delta$ at RT and T_m , conductivity at RT (σ_{RT}) and Curie constant (K) are given in **Table 2**.

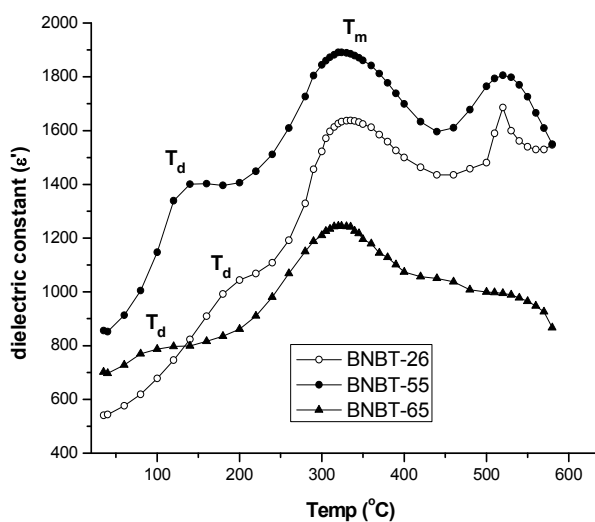
The frequency dependence of the real part of the dielectric constant for BNBT-65 is depicted in **Figure 5** for various temperatures. Two different regions are distinguishable from the **Figure 5(a)**: a plateau region in the high frequency part and a strong dispersion in low frequency region. This phenomenon is commonly observed in conducting materials and is referred to as low frequency dielectric dispersion (LFDD) [34-39]. The same trend has been observed in the remaining compositions BNBT-26 and BNBT-55 as shown in insert **Figures 5(a,b)**. The observed dispersion of the imaginary dielectric constant (ϵ'') (**Figure 5**) is stronger than that of ϵ' . Slope of the curve ϵ'' Versus frequency (f) is found to be close to -1 in low frequency region, which describes the predominance of the dc conduction. In the high frequency region slope lies between 0 and -1, depending on temperature, as it is observed.

According to the Jonscher's power law, the complex dielectric constant as a function of frequency, ω can be expressed as,

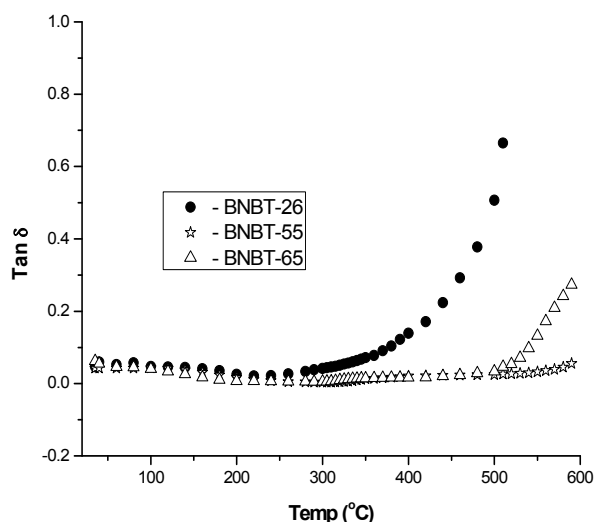
$$\epsilon^* = \epsilon_r' - \epsilon_r'' = \epsilon_\infty + \left(\frac{\sigma}{i\epsilon_0\omega} \right) + \left(\frac{a(T)}{\epsilon_0} \right) (i\omega^{n(T)-1}) \quad (2)$$

From the above equation the real and imaginary parts of ϵ' and ϵ'' can be written as

$$\epsilon_r' = \epsilon_\infty + \sin(n(T)) \frac{\pi}{2} \left(\frac{a(T)}{\epsilon_0} \right) (\omega^{n(T)-1}) \quad (3)$$



(a)



(b)

Figure 4. Variation of (a) ϵ' and (b) $\tan \delta$ of BNBT as a function of temperature.

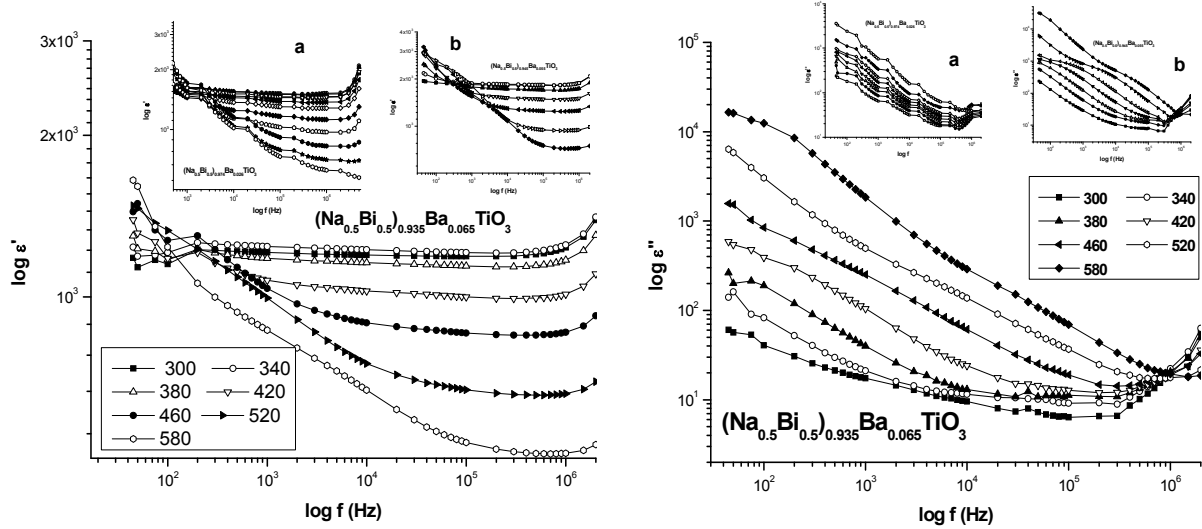


Figure 5. Frequency dependence of ϵ' and ϵ'' at various temperatures.

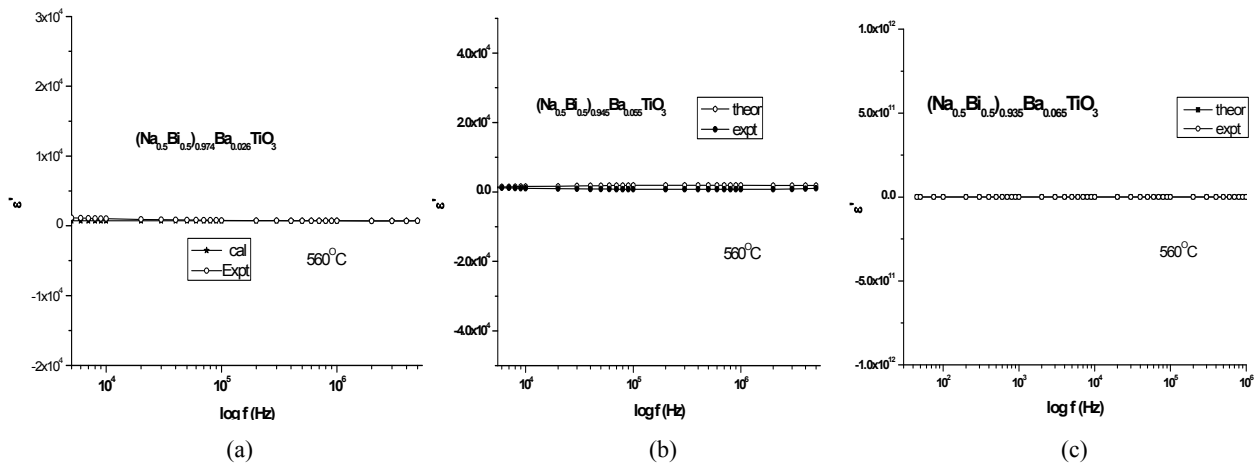


Figure 6. Fitting curves of dielectric constant as a function of frequency at 560 °C.

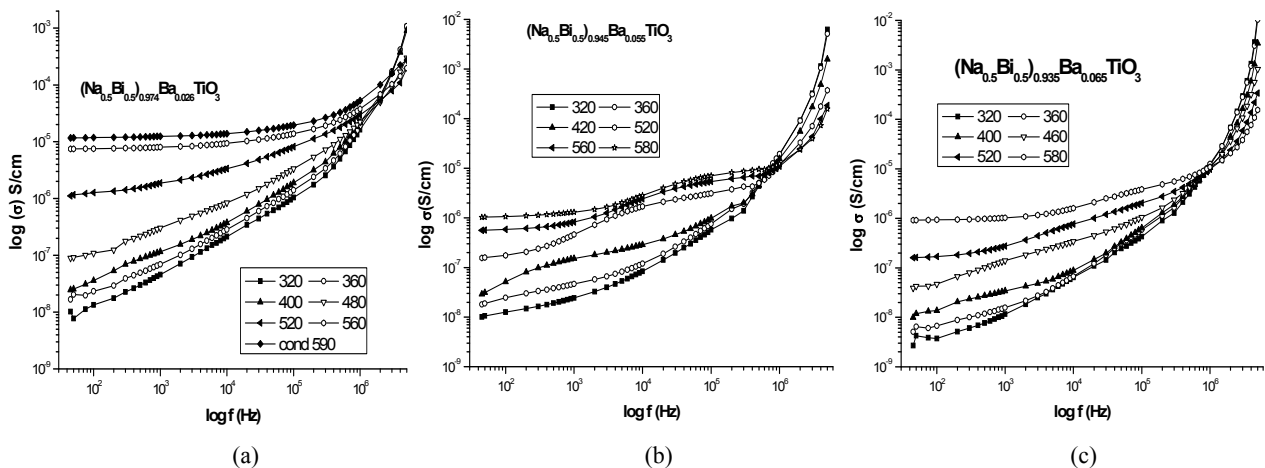


Figure 7. A.C. conductivity as function of frequency at different temperatures of BNBT system.

$$\varepsilon_r'' = \frac{\sigma}{\varepsilon_0 \omega} + \cos(n(T) \frac{\pi}{2}) \left(\frac{a(T)}{\varepsilon_0} \right) (\omega^{n(T)-1}) \quad (4)$$

where ε_∞ is the 'high frequency' value of the dielectric constant, $n(T)$ is the exponent factor, $a(T)$ is prefactor.

Substituting the values of $n(T)$ and $a(T)$ obtained from conductivity measurement in **Eq.3** the theoretical values of ε' has been calculated in the compositions. As the dispersion is negligibly small at higher frequencies, so that the ε_∞ value was chosen as the dielectric constant obtained at 1 MHz. In the studied material the experimental dielectric data have been fitted with theoretical one. The real part of the dielectric constant (ε') at 560°C and theoretically calculated ε' values for BNBT system as a function of frequency is shown in **Figure 6**. It is seen from the **Figure 6** an excellent agreement between experimental and theoretical values for ε' is observed.

4.4. Conductivity Studies

Figure 7 shows the variation of A.C. conductivity as a function of frequency at different temperatures in BNBT-26, BNBT-55 and BNBT-65. The electric conductivity in ceramics is mainly controlled by the migration of charge species under the action of electric field and by the defect-ion complexes, the polarization field, the relaxation etc. In BNBT-65 the high conductivity is observed where as low conductivity is seen in BNBT-26. The observed high conductivity in BNBT-65 is attributed to the presence of oxygen vacancies and low conductivity in BNBT-26 may be due to an enhancement in barrier properties, suppression of lattice conduction path and local lattice distortion [40-42]. Present BNBT system showed a low frequency dielectric dispersion (LFDD) behavior (discussed in Dielectric analysis). The $\sigma(\omega)$ curves are found to be merging at high frequency and temperature regions, suggesting the less defect mobility and low conductivity in the material. The phenomenon of the conductivity dispersion in the materials is generally analyzed by using A.K. Jonscher's law [43]

$$\sigma(\omega) = \sigma_{dc} + A\omega^n \quad (5)$$

where σ_{dc} is the d.c. conductivity for a particular temperature, n is the power law exponent which varies between 0 and 1 depending on temperature and A is the temperature dependent constant.

The $n(T)$ and $A(aS/L)$ are determined from curve fitting using the **Eq.3**. Temperature dependence of both $n(T)$ and $A(aS/L)$ are shown in **Figures 8(a)** and **(b)** respectively. An interesting feature of **Figure 8** is that the two linear regions have been observed in the studied materials corresponding to the paraelectric and ferroelectric states [44-46]. The value of exponent n value is found to decrease with increasing temperature and shows a minimum near T_m . Similar results have been reported in $\text{SrBi}_2\text{Nb}_2\text{O}_9$ (SBN) and $\text{BaBi}_2\text{Nb}_2\text{O}_9$ (BBN) ceramics

[47,48]. The value of prefactor A shows a maximum in the temperature range where n shows a minimum and it decreases with increasing in temperature. According to many body interaction models [43], the interaction between all dipoles participating in the polarization process is characterized by the parameter n . $n = 1$ implies a pure Debye case, where the interaction between the neighboring dipoles is almost negligible. The value of $n(T)$ is observed to be less than one in the studied compositions indicating non-Debye type. The observed minimum $n(T)$ in the vicinity of T_m shows a large extent of interaction between the charge carriers and polarization. The higher value of A in the vicinity of T_m establishes the presence of higher polarizability.

In the materials, the conductivity is found to be independent of frequency at any temperature under study is taken as d.c. conductivity. Here, d.c. conductivity indicates hopping of charge carriers after the surrounding environment has relaxed. The jump relaxation theory introduced by Funke (1993) is to account for ionic conduction in solids. The jump relaxation theory yields the Almond-West assumption, from which the A.C. and d.c. conductivity activation energies are evaluated in the present compositions. The A.C. conductivity is found to obey the Almond-West relation [49].

$$\sigma(\omega) = \sigma_{dc} (1 + \omega_p / \omega)^n \quad (6)$$

where ω_p is the hopping frequency, the ω_p is the transition region between d.c. and A.C. conductivity.

There have been many attempts [50] to relate σ_{dc} to the A.C. conductivity. Whether they are able to do so in equal numbers is not known but it might be expected that effects such as the blocking of conduction pathways. If anything, lead to fewer ions contributing to the d.c. conductivity than to the A.C. conductivity. The relationship between A and σ :

$$\sigma_{dc} = A\omega_p^n \quad (7)$$

was obtained [51] by taking the assumptions that the electrical response, **Eq.5** is a characteristic of the dynamics of the hopping ions and that the same number of ions contributes to the A.C. and d.c. conductivities. It is well known that ω_p is activated with activation enthalpy, H_m followed by the relation $\omega_p = \omega_c \exp(-H_m/k_B T)$. **Figure 9** shows the typical Arrhenius plot of ω_p for BNBT-65. From these plots the value of $H_m = 0.37\text{eV}$, 0.26eV and 0.25eV has been estimated for BNBT-26, BNBT-55 and BNBT-65 respectively. Activation enthalpy (H_m) is decreasing with increasing the concentration of the Ba. The value of H_m is lowest for BNBT-65 which is in MPB region.

The conductivity (d.c and A.C) behavior in the BNBT system has been shown in **Figure 10**. The conductivity of the materials has been found to increase with increase in temperature, representing the negative temperature coefficient of resistance (NTCR) behavior like semiconductors,

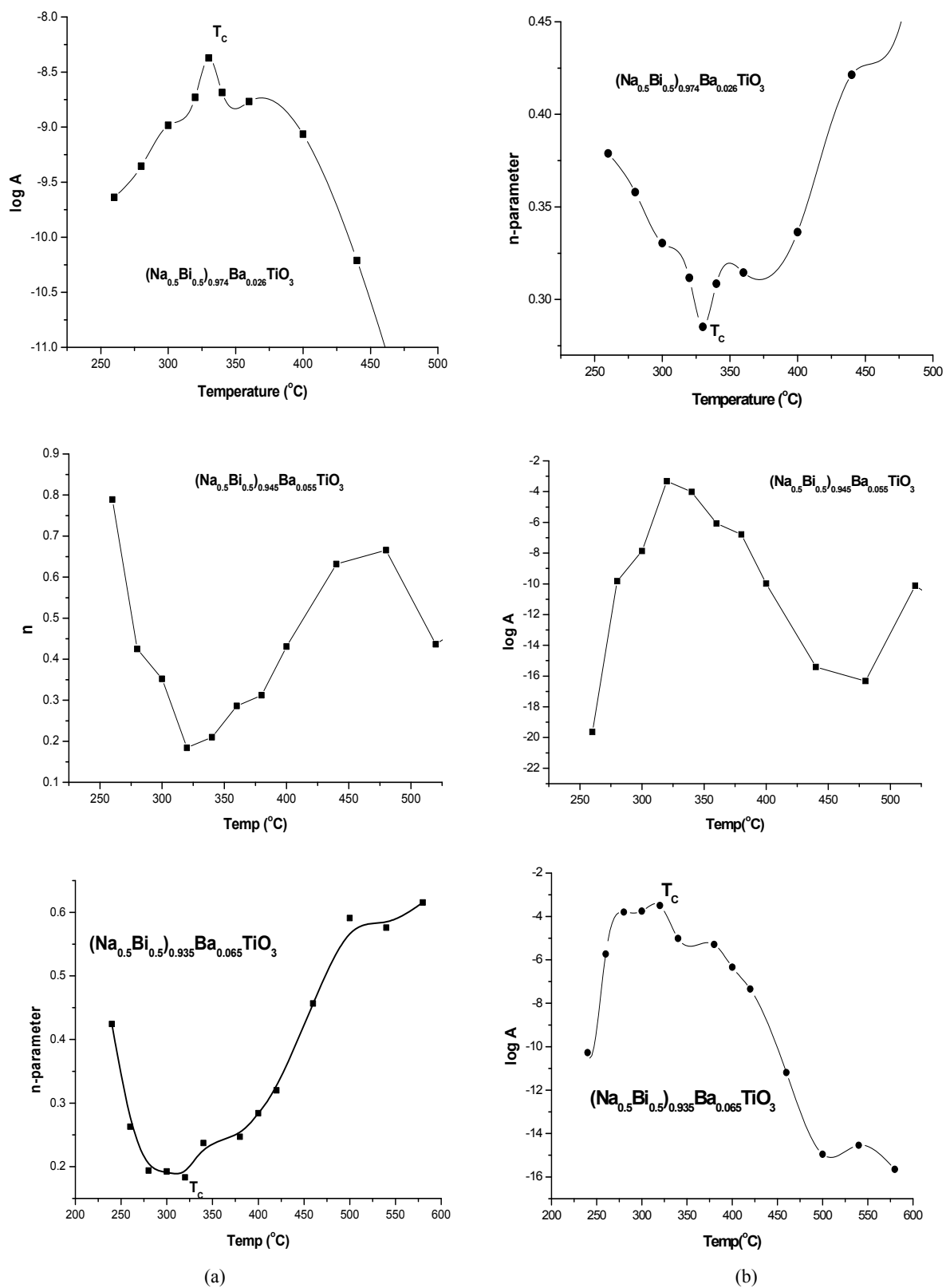


Figure 8. Temperature dependence of (a) $n(T)$ and (b) $A(T)$ parameters of BNBT system.

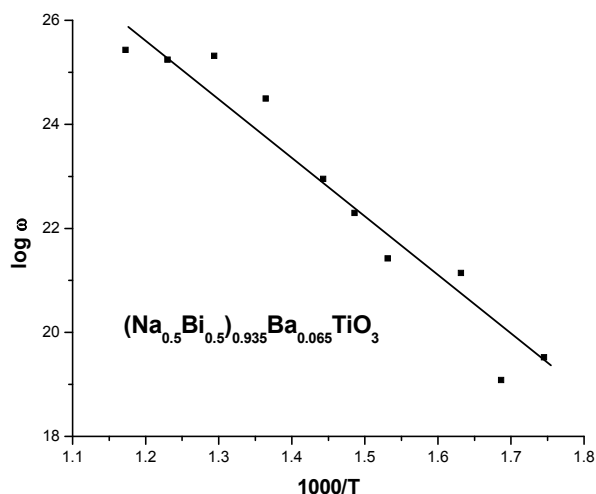


Figure 9. $\log \omega$ as a function of inverse temperature of BNBT-65.

and it is related to the bound carriers trapped in the sample. Merging of all conductivity curves at higher temperature region results the release of space charge [52,53]. At low temperature, the thermal energy is enough to allow migration of atoms/ions into (oxygen) vacancies already associated in the compound. Hence no clear anomalies appeared in this region. The conductivity values at room temperature are 1.38×10^{-8} (s/cm), 2.02×10^{-8} (s/cm), 2.46×10^{-8} (s/cm) for BNBT-26, BNBT-55 and BNBT65 respectively. It is evident that the conductivity is basically due to the oxygen vacancies. High conductivity is observed in BNBT-65 may be due to it is in MPB region. It represents contribution of the reorientation of Ba^{2+} and Ti^{4+} ions coupling with the thermally activated conduction electrons appear due to ionization of the oxygen vacancies in MPB region.

The A.C. and d.c. conduction activation energies have been calculated from different temperature regions (580-470°C, 470-370°C and 370-300°C) (Figures 10(a, b, c)) and at different frequencies using Arrhenius relation $\sigma =$

$\sigma_{\text{dc}} \exp (E_{\text{a}}/K_{\text{B}}T)$ and the obtained values are given in **Table 3**. The activation energy in BNBT-65 is found to be high since it is in MPB region, compare to the other two samples. *i.e.*, below MPB (BNBT-26) and near MPB (BNBT-55). It is seen from the **Figure 10** that a change in the slope of conductivity vs. temperature response of the materials has been observed around the transition temperature may be due to the difference in the activation energy in the ferroelectric and paraelectric regions. This difference in activation energies could be due to the grain boundary effect [54].

The low activation energies found at low temperature and high frequency range in the studied materials suggest the intrinsic conduction may be due to the creation of large number of charge carriers. AC and dc activation energy values at different frequencies and temperature are given in **Table 3**.

5. CONCLUSIONS

The polycrystalline $(\text{Na}_{0.5}\text{Bi}_{0.5})_{1-x}\text{Ba}_x\text{TiO}_3$ ($x = 0.026, 0.055 \text{ \& } 0.065$) (BNBT) ceramics have been synthesized by conventional solid state sintering technique. The tolerance factors (0.988, 0.99 and 0.991) in the studied materials are found to lie well within the limit indicating the materials belong to stable perovskite structure. X-ray powder diffraction patterns of the materials have been indexed and found to be single phase with rhombohedral structure. The evaluated lattice parameters are 3.886Å, 3.891Å and 3.892Å for BNBT-26, BNBT-55 and BNBT-65 respectively. The value of T_{m} and T_{d} are found to decrease with increase of concentration of Barium in BNT. The $\tan \delta$ values in the studied materials are found to be the order of 10^{-2} indicating low loss materials. The evaluated Curie constant in the compositions is found to be the order of 10^5 revealing the materials belong to oxygen octahedra ferroelectrics. A strong low frequency dielectric dispersion has been observed in the studied materials.

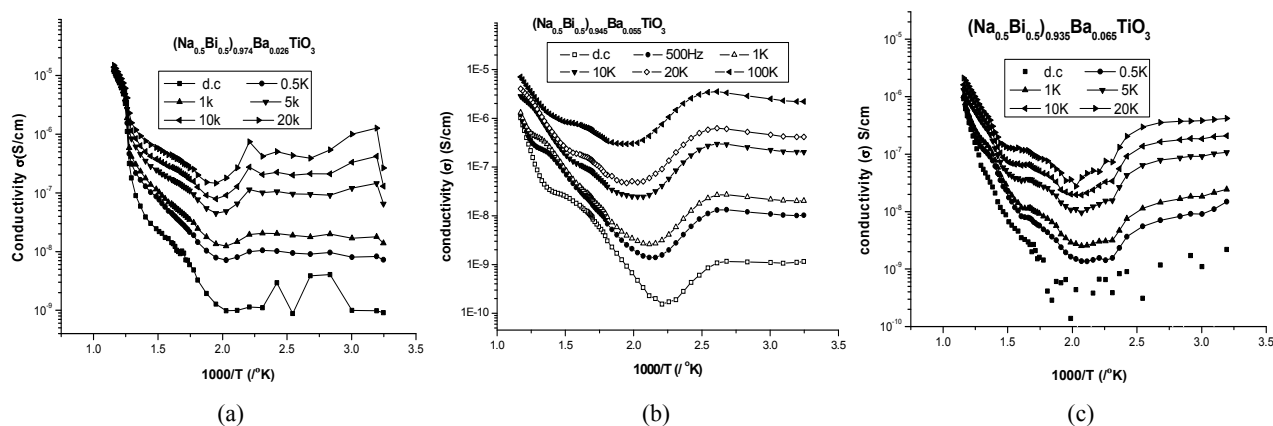


Figure 10. Conductivity vs. inverse temperature of BNBT-system.

Table 3. Activation energies of BNBT materials.

Composition Temperature range	BNBT-26 (eV)			BNBT-55 (eV)			BNBT-65 (eV)		
	d.c	1kHz	10kHz	d.c	1kHz	10kHz	d.c	1kHz	10kHz
580-470	0.49	0.45	0.37	0.5	0.43	0.43	0.66	0.43	0.32
470-370	0.27	0.21	0.15	0.14	0.31	0.38	0.48	0.41	0.39
370-300	0.24	0.15	0.11	0.07	0.22	0.17	0.20	0.23	0.11

The experimental and theoretical dielectric constant (ϵ') are fitted well to the Jonscher's power law. The interaction between the charge carriers, exponent $n(T)$ and strength of polarizability, $A(T)$ are observed to be minimum and maximum at T_m respectively. The value of $n(T)$ is observed to be < 1 in the studied compositions indicating non-Debye type. The electrical relaxation process occurring in the materials are observed to be temperature dependent. Temperature dependence of dc conductivity in the compositions exhibits the NTCR behavior. The d.c. conductivity behaviour in the materials indicates hopping of charge carriers after the surrounding environment has relaxed. The value of activation enthalpy (H_m) are evaluated and found to be 0.37eV, 0.26eV and 0.25 eV for BNBT-26, BNBT-55 and BNBT-65 respectively.

6. ACKNOWLEDGEMENTS

Authors K.S. Rao and K.Ch. VaradaRajulu thank to Naval Science & Technological Laboratory (NSTL)-Visakhapatnam, INDIA for the sanction of a Research Project and providing Research Assistant fellowship.

REFERENCES

- [1] Gomah-Pettry, J.R., Marchet, P., Salak, A., Ferreira, V.M. and Mercurio, J.P. (2004) Electrical properties of $\text{Na}_{0.5}\text{Bi}_{0.5}\text{TiO}_3\text{-SrTiO}_3$ ceramics. *Integrated Ferroelectrics*, **61(1)**, 159-162.
- [2] Nageta, H., Yoshida, M., Makiuchi, Y. and Takenaka, T. (2003) Large piezoelectric constant and high curie temperature of lead-free piezoelectric ceramic ternary system based on bismuth sodium titanate-bismuth potassium titanate-barium titanate near the morphotropic phase boundary. *Japanese Journal of Applied Physics*, **42**, 7401-7403.
- [3] Takenaka, T. and Nagata, H. (2005) Current status and prospects of lead-free piezoelectric ceramics. *Journal of the European Ceramic Society*, **25(12)**, 2693-2700.
- [4] Herabut, A. and Safari, A. (1997) Processing and electromechanical properties of $(\text{Bi}_{0.5}\text{Na}_{0.5})(1-1.5x)\text{LaxTiO}_3$ ceramics. *Journal of the American Ceramic Society*, **80(11)**, 2954-2958.
- [5] Ishii, H., Nagata, H. and Takenaka, T. (2001) Morphotropic phase boundary and electrical properties of bismuth sodium titanate-potassium niobate solid-solution ceramics. *Japanese Journal of Applied Physics*, **40(9B)**, 5660-5663.
- [6] Peng, C., Li, J.F. and Gong, W. (2005) Preparation and properties of $(\text{Bi}_{1/2}\text{Na}_{1/2})\text{TiO}_3\text{-Ba}(\text{Ti},\text{Zr})\text{O}_3$ lead-free piezoelectric ceramics. *Materials Letters*, **59(12)**, 1576-1580.
- [7] Chu, B.J., Chen, D.-R., Li, G.-R. and Yin, Q.-R. (2002) Electrical properties of $\text{Na}_{1/2}\text{Bi}_{1/2}\text{TiO}_3\text{-BaTiO}_3$ ceramics. *Journal of the European Ceramic Society*, **22(13)**, 2115-2121.
- [8] West, D.L. and Payne, D.A. (2003) Preparation of $0.95\text{Bi}_{1/2}\text{Na}_{1/2}\text{TiO}_3\cdot 0.05\text{BaTiO}_3$ ceramics by an aqueous citrate-gel route. *Journal of the American Ceramic Society*, **86(1)**, 192-194.
- [9] Kimura, T., Takahashi, T., Tani, T. and Saito, Y. (2004) Preparation of crystallographically textured $\text{Bi}_{0.5}\text{Na}_{0.5}\text{TiO}_3\text{-BaTiO}_3$ ceramics by reactive-templated grain growth method. *Ceramics International*, **30(7)**, 1161-1167.
- [10] Xu, Q., Chen, S.T., Chen, W., Wu, S.J., Zhou, J., Sun, H.J. and Li, Y.M. (2005) Synthesis and piezoelectric and ferroelectric properties of $(\text{Na}_{0.5}\text{Bi}_{0.5})(1-x)\text{BaxTiO}_3$ ceramics. *Materials Chemistry and Physics*, **90(1)**, 111-115.
- [11] Gao, L., Huang, Y., Hu, Y. and Du, H. (2007) Dielectric and ferroelectric properties of $(1-x)\text{BaTiO}_3\text{-xBi}_{0.5}\text{Na}_{0.5}\text{TiO}_3$ ceramics. *Ceramic International*, **33(6)**, 1041-1046.
- [12] Qu, Y., Shan, D. and Song, J. (2005) Effect of A-site substitution on crystal component and dielectric properties in $\text{Bi}_{0.5}\text{Na}_{0.5}\text{TiO}_3$ ceramics. *Materials Science and Engineering B*, **121(1-2)**, 148-151.
- [13] Shannon, R.D. (1976) Revised effective ionic radii and systematic studies of interatomic distances in halides and chalcogenides. *Acta Crystallographica Section A*, **32**, 751-767.
- [14] Muller, O. and Roy, R. (1974) The major ternary structural families. Springer, New York, 221.
- [15] Bhalla, A.S., Guo, R. and Roy, R. (2000) The perovskite structure—a review of its role in ceramic science and technology. *Materials Research Innovations*, **4(1)**, 3-26.
- [16] Eitel, R.E., Randall, C.A., Shrout, T.R. and Rehrig, P.W. (2001) New high temperature morphotropic phase boundary piezoelectrics based on $\text{Bi}(\text{Me})\text{O}_3\text{-PbTiO}_3$ ceramics. *Japanese Journal of Applied Physics*, **40(10)**, 5999-6002.
- [17] Reaney, I.M., Colla, E.L. and Setter, N. (1994) Dielectric and structural characteristics of Ba-based and Sr-based complex perovskites as a function of tolerance factor. *Japanese Journal of Applied Physics*, **33(7A)**, 3984-3990.
- [18] Suchomel, M.R. and Davies, P.K. (2004) Predicting the position of the morphotropic boundary in new high temperature $\text{PbTiO}_3\text{-Bi}(\text{B}'\text{B}'')\text{O}_3$ based dielectric ceramics. *Journal of Applied Physics*, **96(8)**, 4405-4410.
- [19] Isupov, V.A. (2005), Ferroelectric $\text{Na}_{0.5}\text{Bi}_{0.5}\text{TiO}_3$ and $\text{K}_{0.5}\text{Bi}_{0.5}\text{TiO}_3$ perovskites and their solid solutions. *Ferroelectrics*, **315(1)**, 123-147.
- [20] Park, S.E. and Chung, S.J. (1994), Phase transition of ferroelectric $(\text{Na}_{1/2}\text{Bi}_{1/2})\text{TiO}_3$ on applications of ferroelectrics. *Proceedings of the 9th IEEE International Symposium, ISAF'94*, 265-268.
- [21] Liu, Y.F., Lv, Y.N., Xu, M., Shi, S.Z., Xu, H.Q. and

- Yang, X.D. (2007) Structure and electric properties of $(1-x)(\text{Bi}_{1/2}\text{Na}_{1/2})\text{TiO}_3-x\text{BaTiO}_3$ systems. *Journal of Wuhan University of Technology - Materials Science Edition*, **22(2)**, 315-319.
- [22] Mahboob, S., Prasad, G. and Kumar, G.S. (2007) Impedance spectroscopy and conductivity studies on B site modified $(\text{Na}_{0.5}\text{Bi}_{0.5})(\text{Nd}-x\text{Ti}(1-2x)\text{Nbx})\text{O}_3$ ceramics. *Journal of Material Science*, **42**, 10275-10283.
- [23] Takenaka, T. (1999) Piezoelectric properties of some lead-free ferroelectric ceramics. *Ferroelectrics*, **230**, 87-98.
- [24] Liu, Y.F., et al. (2007) *Journal of Wuhan University of Technology - Materials Science Edition*.
- [25] Takenaka, T. (1989) Piezoelectric properties of some lead-free ferroelectric ceramics. *Ferroelectrics*, **230**, 389.
- [26] Yoshii, K., Nagata, H. and Takenaka, T. (2006) Electrical properties and depolarization temperature of $(\text{Bi}_{1/2}\text{Na}_{1/2})\text{TiO}_3-(\text{Bi}_{1/2}\text{K}_{1/2})\text{TiO}_3$ lead-free piezoelectric ceramics. *Japanese Journal of Applied Physics*, **45**, 4493.
- [27] Takenaka, T., Okuda, T. and Takegahara, K. (1997) Lead-free piezoelectric ceramics based on $(\text{Bi}_{1/2}\text{Na}_{1/2})\text{TiO}_3-\text{NaNbO}_3$. *Ferroelectrics*, **196**, 175.
- [28] Li, H.D., Feng, C.D. and Yao, W.L. (2005) Some effects of different additives on dielectric and piezoelectric properties of $(\text{Bi}_{0.5}\text{Na}_{0.5})\text{TiO}_3-\text{BaTiO}_3$ morphotropic phase boundary composition. *Materials Letters*, **58**, 1194-1198.
- [29] Nagata, H. and Takenaka, T. (2001) Additive effects on electrical properties of $(\text{Bi}_{1/2}\text{Na}_{1/2})\text{TiO}_3$ ferroelectric ceramics. *Journal of European Ceramic Society*, **21**, 1299.
- [30] Wei, Z., Heping, Z. and Yongke, Y., et al. (2007) Dielectric and piezoelectric properties of Y_2O_3 doped $(\text{Bi}_{0.5}\text{Na}_{0.5})_{0.94}\text{Ba}_{0.06}\text{TiO}_3$ lead-free piezoelectric ceramics. *Key Engineering Materials*, **105**, 336-338.
- [31] Lin, D., Xiao, D., Zhu, J. and Yu, P. (2006) Piezoelectric and ferroelectric properties of $[\text{Bi}_{0.5}\text{Na}_{1-x-y}\text{K}_x\text{Li}_{y0.5}]\text{TiO}_3$ lead-free piezoelectric ceramics. *Applied Physics Letters*, **88**.
- [32] Tu, C.S., Siny, I.G. and Schimidt, V.H. (1994) Dielectric, NMR and X-Ray diffraction study of $\text{Cs}_{1-x}(\text{NH}_4)_x\text{H}_2\text{PO}_4$. *Physical Review B*, **49**, 11550.
- [33] Chowdury, P.R. and Deshpande, S.B. (1984) *Indian Journal of Pure & Applied Physics*, **22**, 708.
- [34] Jonscher, A.K. and Dube, D.C. (1978) Low frequency dispersion in tri-glycine sulphate. *Ferroelectrics*, **17**, 533-536.
- [35] Jonscher, A.K. (1989) Interpretation of non-ideal dielectric plots. *Journal of Material Science*, **24**, 372.
- [36] Garcia-Martin, S., Veiga, M.L., Pico, C., Santamaria, J., Gonzalez-Diaz, G. and Sanchez-Quesada, F. (1990) Dielectric response and ionic conductivity of $\text{Cs}(\text{NbTe})\text{O}_6$. *Materials Research Bulletin*, **25**, 1393.
- [37] Jonscher, A.K., Deori, K.L., Reau, J.M. and Moali, J. (1979) The dielectric response of $\text{K}_x\text{Al}_x\text{Ti}_{8-x}\text{O}_{16}$ and $\text{K}_x\text{Mg}_{x/2}\text{Ti}_{8-x/2}\text{O}_{16}$. *Journal of Materials Science*, **14**, 1308-1320.
- [38] Garcia-Martin, S., Veiga, M.L., Pico, C., Santamaria, J., Gonzalez-Diaz, G. and Sanchez-Quesada, F. (1990) Barrier effects on ionic conductivity and dielectric response of $\text{Ti}(\text{NbTe})\text{O}_6$. *Solid State Ionics*, **44**, 131.
- [39] Varez, A., Alario-Franco, M.A., Santamaria, J., Gonzalez-Diaz, G. and Sanchez-Quesada, F. (1990) Ionic conductivity of lithium inserted $\text{Ba}_{2y}\text{Cu}_3\text{O}_{7-y}$. *Solid State Communications*, **76(7)**, 917-920.
- [40] Kumar, A., Singh, B.P., Choudary, R.N.P. and Thakur, A.K. (2005) A.C. impedance analysis of the effect of dopant concentration on electrical properties of calcium modified BaSnO_3 . *Journal of Alloys and Compounds*, **394(1-2)**, 292-302.
- [41] Scott, B.A., Geiss, E.A., Olson, B.L., Burns, G., Smith, A.W. and O'Kane, D.F. (1970) The tungsten bronze field in the system $\text{K}_2\text{O}|\text{Li}_2\text{O}|\text{Nb}_2\text{O}_5$. *Materials Research Bulletin*, **5(1)**, 47-56.
- [42] Kroger, F.A. and Vink, H.J. (1956) Relations between the concentrations of imperfections in crystalline solids. *Solid State Physics*, **3**, 307.
- [43] Jonscher, A.K. (1983) Dielectric relaxation in solids. Chelsea Dielectric Press, London.
- [44] Henn, F.E.G., Giuntini, J.C., Zanchetta, J.V., Granier, W. and Taha, A. (1990) Frequency dependent protonic conduction in $\text{N}_2\text{H}_5\text{Sn}_3\text{F}_7$ glass and RbHSeO_4 single crystal. *Solid State Ionics*, **42(1-2)**, 29-36.
- [45] Giuntini, J.C., Deroide, B., Belougne, P. and Zanchetta, J.V. (1987) Numerical approach of the correlated barrier hopping model. *Solid State Communications*, **62**, 739.
- [46] Bensimon, Y., Giuntini, J.C., Belougne, P., Deroide, B. and Zanchetta, J.V. (1988) *Solid State Communications*, **68**, 189.
- [47] Venkataraman, B.H. and Varma, K.B.R. (2004) Frequency-dependent dielectric characteristics of ferroelectric $\text{SrBi}_2\text{Nb}_2\text{O}_9$ ceramics. *Solid State Ionics*, **167**, 197-202.
- [48] Krthik, C. and Varma, K.B.R. (2006) Dielectric and AC conductivity behavior of $\text{BaBi}_2\text{Nb}_{209}$ ceramics. *Journal of Physics and Chemistry of Solids*, **67(12)**, 2437-2441.
- [49] Almond, D.P. and West, A.R. (1983) Mobile ion concentrations in solid electrolytes from an analysis of a.c. conductivity. *Solid State Ionics*, **22**, 277.
- [50] Hill, R.M. and Jonscher, A.K. (1979) *Journal of Non-Crystalline Solids*, **32**, 53.
- [51] Almond, D.P., West, A.R. and Grant, R.J. (1982) Temperature dependence of the a.c. conductivity of $\text{Na}\beta$ -alumina. *Solid State Communications*, **44(8)**, 1277-1280.
- [52] Sundarkannan, S., Kakimoto, K. and Ohsato, H. (2003) *Journal of Applied Physics*, **9**, 5182.
- [53] Lu, Z., Bonnet, J.P., Ravez, J. and Hagenmuller, P. (1992) Correlation between low frequency dielectric dispersion (LFDD) and impedance relaxation in ferroelectric ceramic $\text{Pb}_2\text{KNb}_4\text{TaO}_{15}$. *Solid State Ionics*, **57(3-4)**, 235-244.
- [54] Thakur, O.P. and Prakash, C. (2003) Dielectric properties of samarium substituted barium strontium titanate. *Phase Transformation*, **76(6)**, 567-574.